ISTITUTO NAZIONALE DI FISICA NUCLEARE

Sezione di Milano

INFN/BE-81/11
29 Giugno 1981

P. Guazzoni, I. Iori, P. Michelato, A. Moroni, G. F. Taiocchi and L. Zetta: AN ELECTRONIC DEVICE FOR PARTICLE IDENTIFICATION AND ENERGY SPECTRA ACQUISITION.

Servizio Documentazione
dei Laboratori Nazionali di Frascati

Istituto Nazionale di Fisica Nucleare
Sezione di Milano

INFN/BE-81/11
29 Giugno 1981

AN ELECTRONIC DEVICE FOR PARTICLE IDENTIFICATION AND ENERGY SPECTRA ACQUISITION

P. Guazzoni, I. Iori, P. Michelato, A. Moroni, L. Zetta
INFN, Sezione di Milano, and Istituto di Fisica dell'Università di Milano

and

G. F. Taiocchi
Ditta Takes, Ponteranica Bergamo

ABSTRACT

This report represents the user guide for a new analog device, able to identify the charged reaction products and to detect the corresponding energy spectra.

1. - INTRODUCTION.

A problem arising in low energy experimental nuclear physics is the identification of charged reaction products and the detection of their energy spectra.

The identification of light charged particles with a silicon detector telescope is based on the different energy loss in the totally depleted transmission counter ΔE.

To manipulate the ΔE and E signals, different algorithms have been suggested[1-3], whose computation may be made hardware and software.

In both cases a standard electronic chain is needed to process the signals before identification, as shown in Fig. 1.

The first device here described, i.e. the identifier, has some new aspects if compared to usual set-ups : in fact it is an instrument simple, compact, reliable and easy to use, so that it may be employed directly after the amplifiers, giving as output the linear $E + \Delta E$, the identifying and

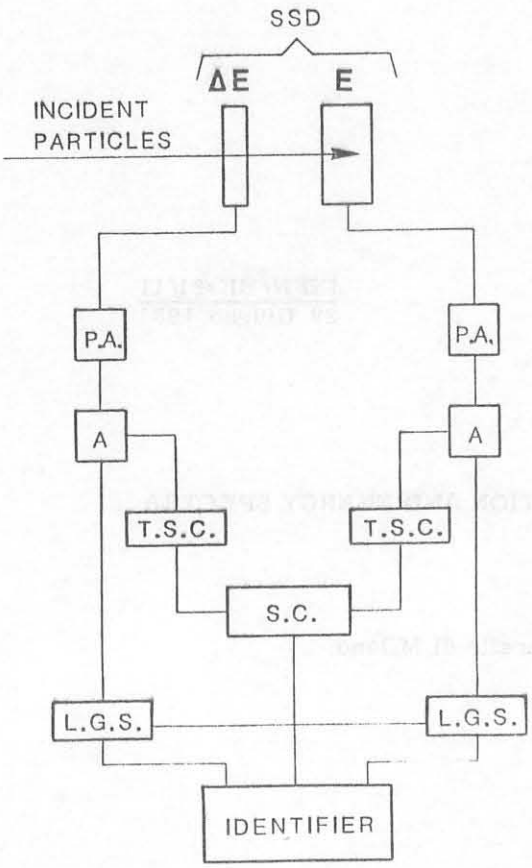

sampling signals. Moreover, the identification function is calculated with an analog computer made by logarithmic and operational amplifiers, allowing a very easy parameter adjustment.

The second device here described, i. e. the window selector, emphasizes the compactness of the identification system, allowing an attainment up to eight energy spectra, corresponding to different particles, with one ADC only of the data acquisition apparatus. Most of the standard electronics usually required, with analog identifiers, to collect different energy spectra, may thus be eliminated.

The present report intends to be, most of all, a user guide of the particle identifier and the window selector modules.

FIG. 1 - Block diagram of a standard telescope identifier system.

2. - ALGORITHM CHOICE AND PARTICLE IDENTIFIER DESCRIPTION.

Many algorithms have been proposed[1-3] to discriminate light charged particles. We have followed the Goulding suggestion[4] based on the empirical range-energy relation $R = a E^x$: this, in fact, seems to be the most convenient for light particle identification and, furthermore, it requires only one adjustable parameter[4], the exponent x.

Being ΔE and E the signals from a detector telescope, following the power law technique, the identifier calculates a Particle Identifier Function $PIF = (E + \Delta E)^x - (E)^x$.

We have designed and built an analog device, able to manipulate four input pulses, E, ΔE, γ, $\bar{E}$, as shown in Fig. 2:

ΔE is the signal corresponding to the energy lost in the thin detector;

E is the signal due to the residual energy lost in the thick detector;

γ (optional) is the signal corresponding to the energy of a possible γ-line in coincidence with the detected particle;

$\bar{E}$ (optional) is the signal from a reject detector, used to minimize the background due to particles of range longer than the telescope thickness.

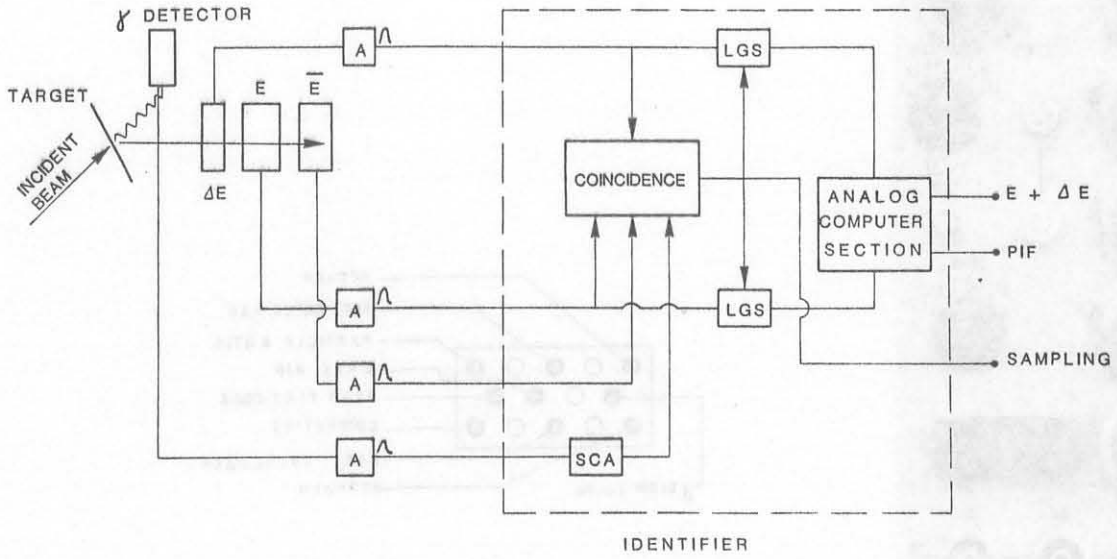

FIG. 2 - Block diagram of present identifier even with both γ and $\bar{E}$ channels.

γ and $\bar{E}$ inputs are used only in particular cases: their role may be seen in Fig. 2. These signals enter the general coincidence only and do affect in no way the identifier operation, which has to deal only with the ΔE and E pulses.

From the amplifiers, the signals E and ΔE follow two paths: a linear and a logic one. The linear channel gives the output signal $E + \Delta E$ (total energy lost in the telescope), for coincident E and ΔE only. The logic one provides the signal (IDENT) corresponding to the identification function, and the sampling signal (SAMP) to the ADC.

The particle identifier is mounted in a standard two units NIM module.

BNC connectors for E, ΔE, γ inputs, $E + \Delta E$, IDENT, SAMP outputs and different control switches are in the front panel (Fig. 3a). These controls are:

a) Identification signal gain: a four position switch for the coarse gain and a ten turn potentiometer for the fine one ($G_{max} = 8$).

b) Exponent: two ten turn potentiometers to adjust both functions $(E + \Delta E)^x$ and $(E)^x$ separately $(0 \leq x \leq 2)$.

c) E, ΔE lower thresholds: two ten turn potentiometers to adjust (0-2 V) both thresholds, independently.

d) E, ΔE delay: two potentiometers to adjust, independently, the time delay of the two input signals (0.5-2 μs).

e) ΔE gain: five position attenuation control (1-0.2) allows the feeding of a ΔE input signal up to five times amplified. This is due to the practical implication that the incident particle generally loses a much smaller fraction of its energy in the ΔE detector than in the E detector.

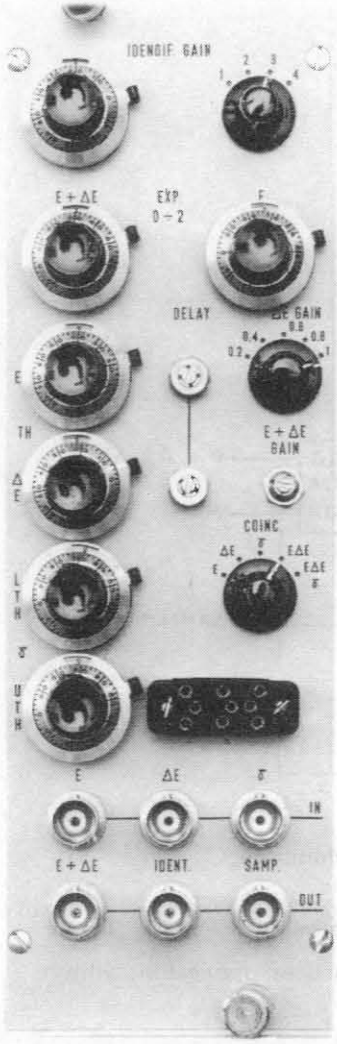

a)

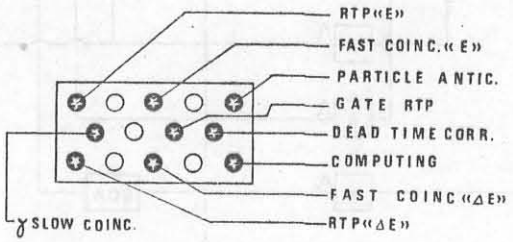

b)

FIG. 3 - a) Photograph of the identifier front view ; b) Test point base.

f) E + ΔE gain : fine adjustement potentiometer (± 10%) for the linear output signal.

g) γ-window : two ten turn potentiometers to adjust the lower and upper thresholds of the γ-channel.

h) Coincidence mode selection : a five position switch to select the data taking mode ; two are for measurement and three for calibration. They are labelled as follows :

Measurement : 1) E + ΔE/γ = E + ΔE, IDENT, SAMP as output signals, only if coincident with selected γ-line ;

2) E + ΔE = output as before but no γ-coincidence required.

Calibration : 1) γ = calibration of the γ-channel. The SAMP output may be sent into the delayed coincidence of an ADC which linear input is the γ-energy pulse ;

2) ΔE = ΔE gain adjustement. With the ΔE input only, one gets the linear ΔE signal, from the linear output (E + ΔE) and the corresponding sampling (SAMP).

3) E = the same as before, but for the E linear signal.

i) Test point base : it enables one to look at the different test signals (Fig. 3b).

The anticoincidence input (GATE) is on the rear, together with its lower threshold, the switch selector (2-8 μs) for the rise time protection and that for the computing time (25-50 μs).

3. - IDENTIFIER BLOCK DIAGRAMS AND OPERATIONAL PRINCIPLES.

The dotted part of the drawing in Fig. 2 is a simplified block diagram of the identifier. The four analog channels E, ΔE, γ, $\bar{E}$ are provided with:

a) 1 kΩ input impedence;

b) lower thresholds for E, ΔE, $\bar{E}$ signals;

c) rise time protections (RTP): they keep the linear gates open and give a first check of the E, ΔE input signals coincidence. In fact, only the pulses reaching their maximum value within the RTP are accepted;

d) peak detectors of the pulse maximum values; they control the adjustable time delays of the E, ΔE pulses;

e) various coincidence circuits controlling the computing time of the analog computer;

f) sampling signal which is activated at the end of the computing time and allows the sampling of the data (E+ΔE, IDENT) in the ADC;

g) stretcher and adder for the linear E, ΔE signals;

h) γ-input peak detector that controls a 3 μs monostable for γ-signal coincidence;

i) 10 μs monostable for the reject channel; it takes part in the general coincidence and it is reset by the computing signal, to minimize the random coincidence background.

Following the block diagram of Fig. 2, operational principles of each section will be described; the corresponding block diagrams are shown in Figs. 4.

Let us follow (Fig. 4a) the path of E and ΔE signals starting from the input connector. The two channel are identical except the presence of the attenuator in the ΔE.

DC levels of the amplifier are cut-off via a passive DC restorer with a large time constant, to avoid integral linearity distortion. The input signal, after a limiter ($\pm$5 V), splits into two operational amplifiers, working as emitter followers, at the start of the linear and logic way, respectively.

The linear signal passes through a linear gate, normally open, closed from the end of the RTP up to the computing completion. Then it passes through a stretcher, acting as an analog buffer, which is controlled, during the charge by the input signal and during the discharge by a fast circuit. This circuit is built with a constant current generator, normally switched off as soon as the threshold goes off.

It remains inhibited up to 1 μs after the sampling signal. Along the logic channel, at first the signal passes through a threshold comparator: when this is busy, processing a signal, an inhibit waveform for the coincidence is generated to prevent the acceptance of further pulses. The RTP then goes off: during this time the peak of the analog signal must arrive, so that the peak detector, used as time base to trigger the delay monostable, starts operating. Now the signal

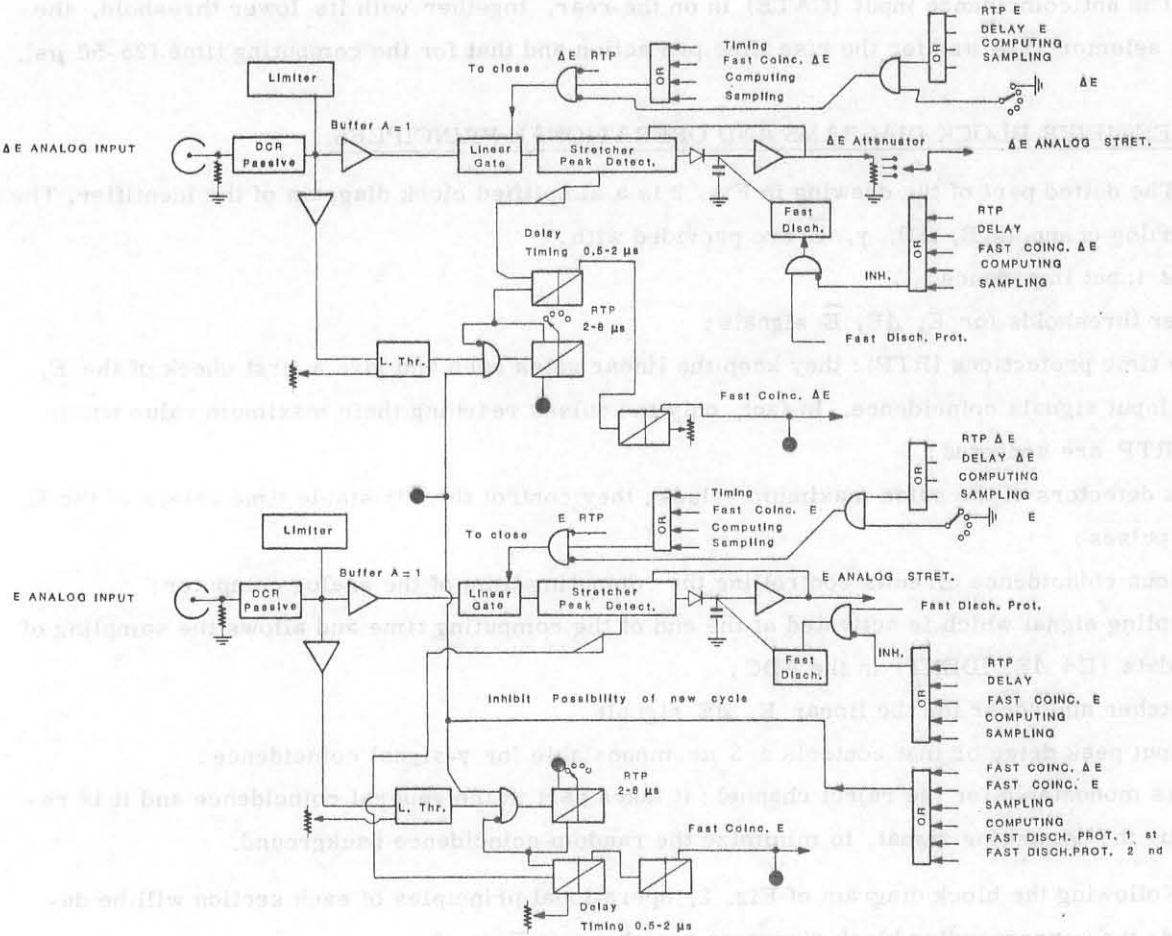

FIG. 4a - Block diagram of the ΔE, E linear and logic input section.

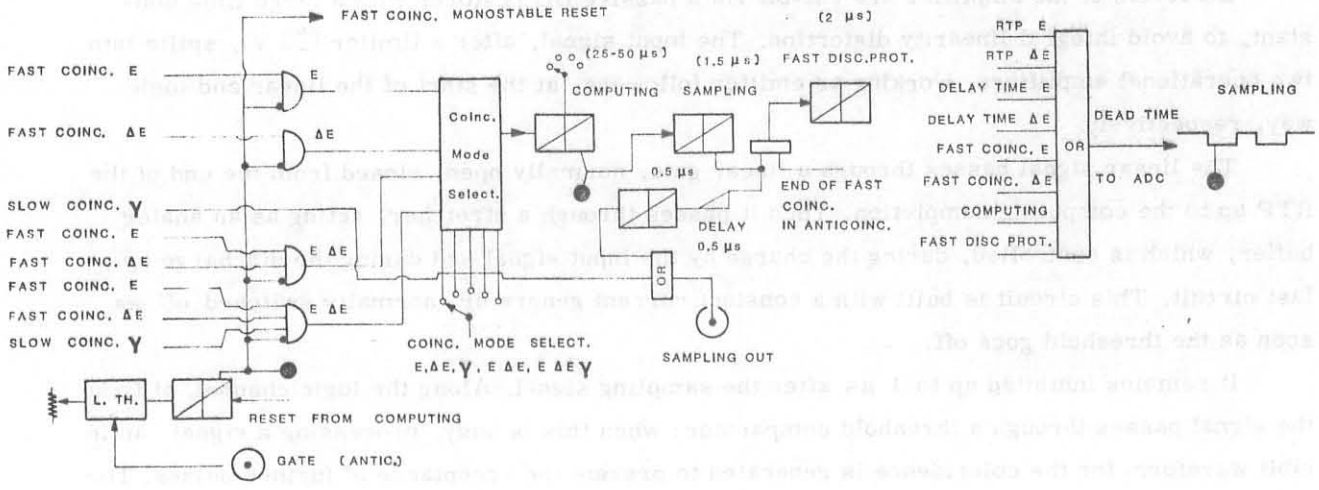

FIG. 4b - Block diagram of the reject channel and general coincidence section.

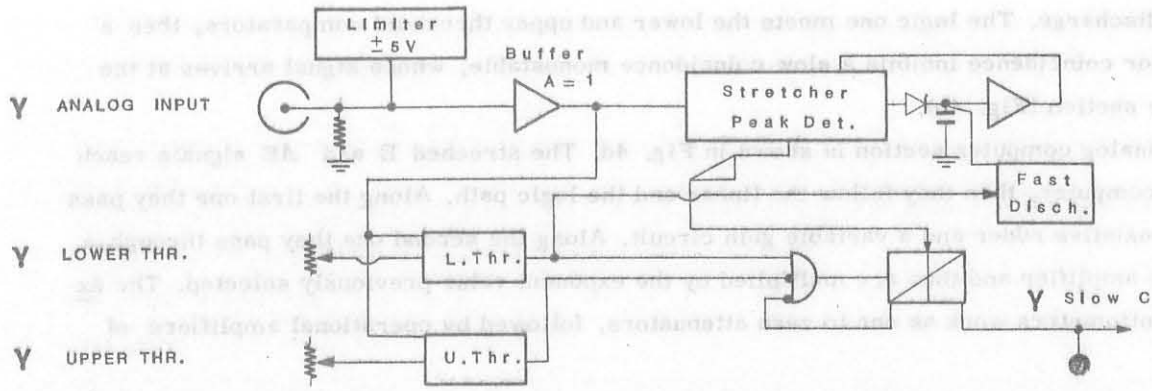

FIG. 4c - Block diagram of the γ-channel logic unit.

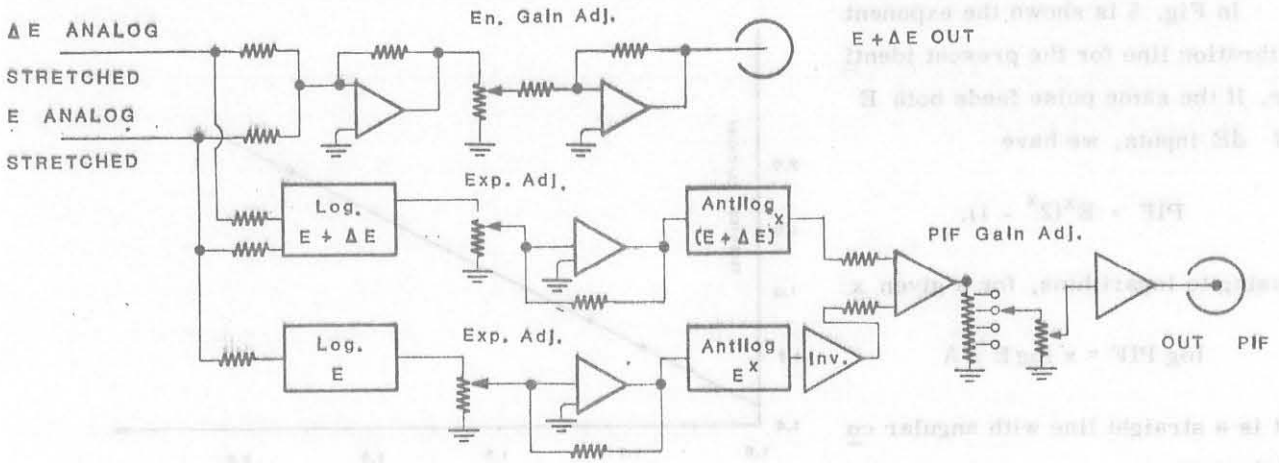

FIG. 4d - Block diagram of the analog computer section.

passes through the coincidence section and the calculation goes on.

The anticoincidence $\bar{E}$ meets (Fig. 4b) at first a lower threshold, then it runs through the coincidence section.

In a similar way, the γ-signal, after a suitable process that will be discussed later (Fig. 4c), will reach the coincidence section. As previously seen, the four analog signal (Fig. 4b) reach the general coincidence that is controlled by the coincidence mode selector. If the anti-coincidence gate is open (i. e. no input greater than the threshold) the coincidence mode selection allows the fast coincidence pulse to trigger the computing monostable. At the end, this one triggers the sampling monostable to generate the output SAMP pulse. The cycle ends with a fast discharge protection which restores the stretcher capacitor.

In order to calibrate the E or ΔE channels independently, it is possible to take out a sampling signal without ΔE or E input, depending on the selected coincidence mode.

The γ-signal (Fig. 4c) after a passive DC restorer enters a buffer with a voltage limiter, then it splits into a linear and a logic path. The linear pulse passes through a stretcher with fast

automatic discharge. The logic one meets the lower and upper threshold comparators, then a peak detector coincidence inhibits a slow coincidence monostable, whose signal arrives at the coincidence section (Fig. 4b).

The analog computer section is shown in Fig. 4d. The streched E and ΔE signals reach the analog computer, then they follow the linear and the logic path. Along the first one they pass through a resistive adder and a variable gain circuit. Along the second one they pass through a logarithmic amplifier and then are multiplied by the exponent value previously selected. The exponent potentiometers work as one to zero attenuators, followed by operational amplifiers of gain two.

Two antilogarithmic amplifiers transform these quantities into $(E)^x$ and $(E+\Delta E)^x$; the first is inverted, then they are summed by means of a resistor adder. Finally the PIF signal arrives at the output connector (IDENT) through an output amplifier, required by its wide range.

In Fig. 5 is shown the exponent calibration line for the present identifier. If the same pulse feeds both E and ΔE inputs, we have

$$PIF = E^x(2^x - 1).$$

Passing to logarithms, for a given x:

$$\log PIF = x \log E + A$$

that is a straight line with angular coefficient x.

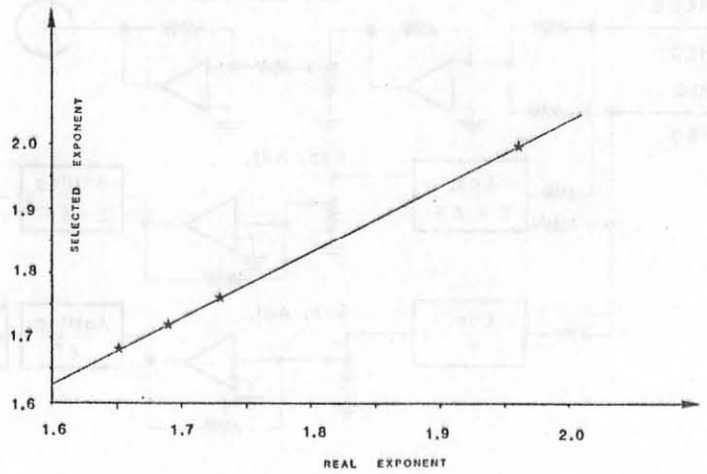

FIG. 5 - Calibration curve for the identification function exponent.

By means of the DAG pulser[5], using 39 pairs of equal pulses, from 100 mV in steps of 100 mV, the corresponding PIF values was measured. The results, analyzed with the linear regression method, are reported in Table I.

TABLE I

Selected x	Real x	Correlation coeff.
1.68	1.649	0.99995
1.72	1.694	0.99991
1.76	1.730	0.99994
2.00	1.965	0.99994

The waveform timing diagrams in the system are shown in Fig. 6.

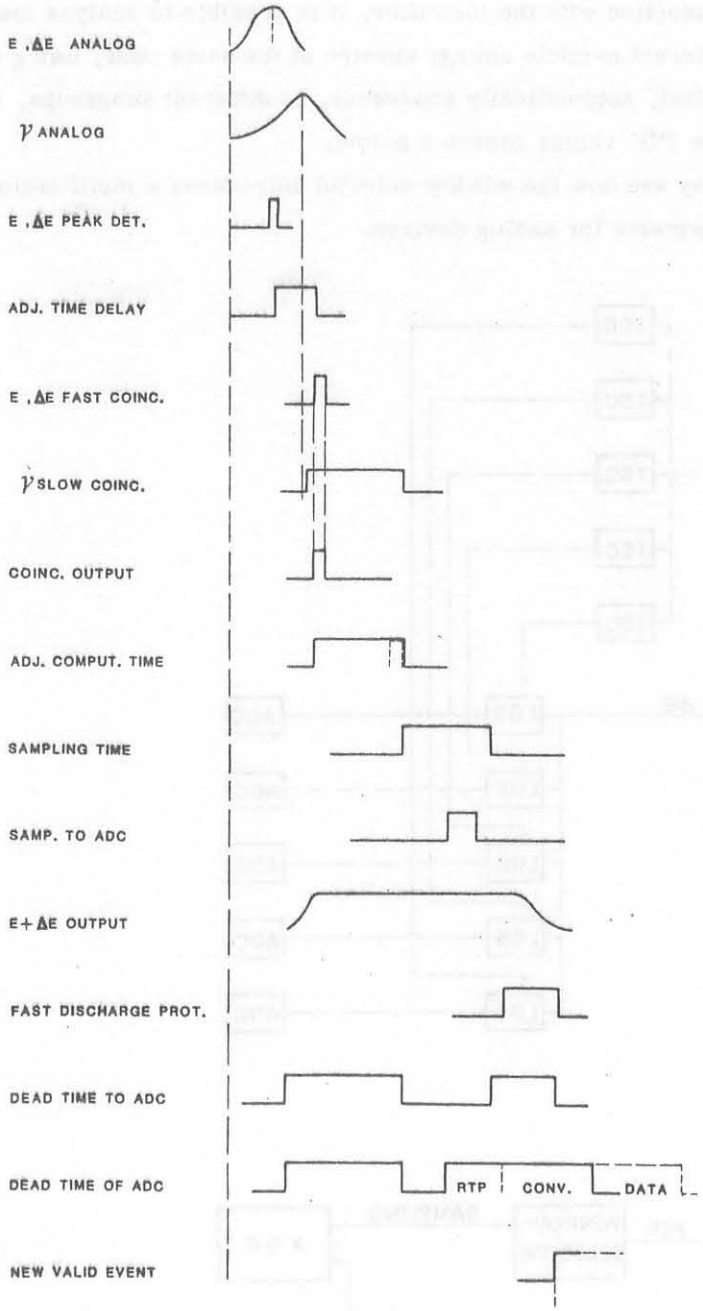

FIG. 6 - Timing of waveform in identifier system.

4. - WINDOW SELECTOR BLOCK DIAGRAMS AND OPERATIONAL PRINCIPLES.

The window selector is mounted in a two units NIM module. By means of its eight contiguous windows, in connection with the identifier, it is possible to analyze the PIF value and to obtain up to eight different particle energy spectra at the same time, using one ADC only.

The selector, in fact, automatically addresses, to different subgroups, the energy spectra corresponding to the PIF values chosen a priori.

In Figs. 7 one may see how the window selector introduces simplification with respect to typical output arrangements for analog devices.

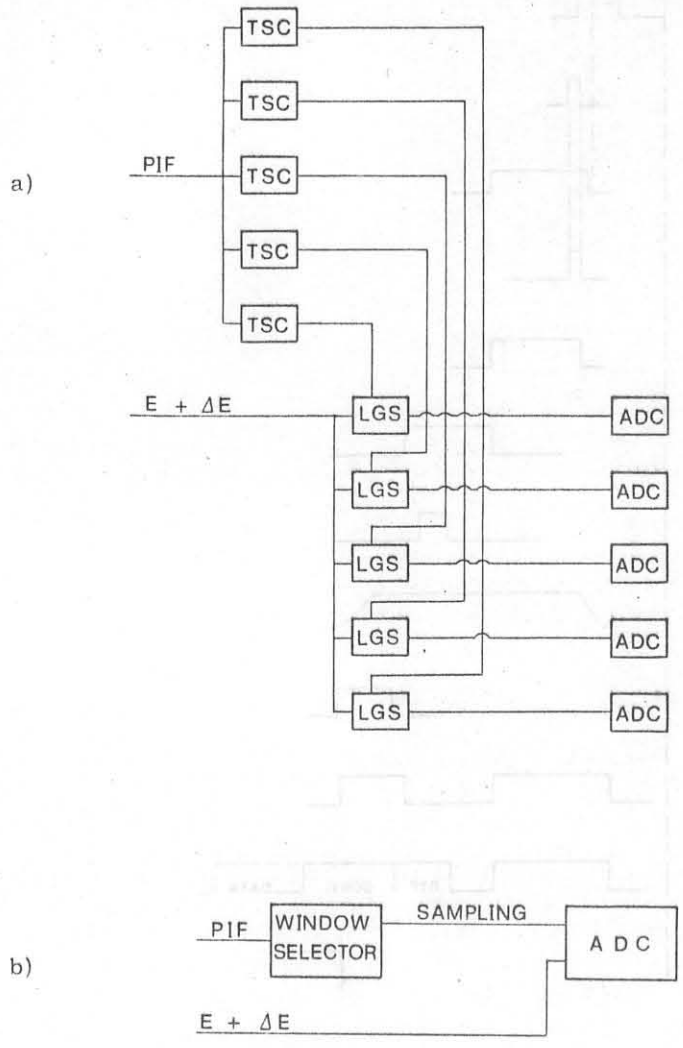

FIG. 7 - a) Block diagram of a standard output electronic chain for energy spectra acquisition with analog identifier. b) Block diagram of the present output section.

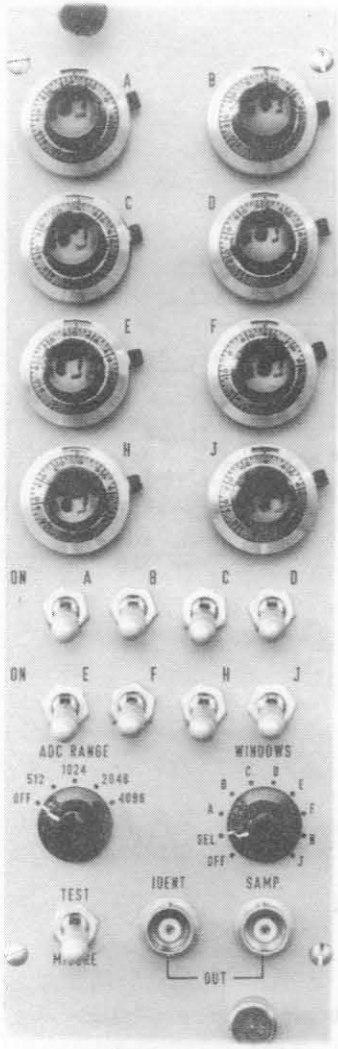

FIG. 8 - Photograph of the window selector front view.

Once the windows of interest are selected, the procedure is as follows :

1) All events falling out of the activated windows are disregarded.
2) The events falling within the first threshold pair selected, enable the corresponding $E + \Delta E$ linear signal to be stored in the first memory subgroup ; the same happens for the second threshold pairs and so on.

Fig. 8 is the front view of the window selector.

The eight ten turn potentiometers are for windows regulation (0-5 V) ; the eight switches enable the different windows (i.e. the first switch enables the events falling between the values of the A and B potentiometers and so on ; the eighth switch enables all the events larger than the J potentiometer value).

The five position switch (ADC RANGE) allows the selection of the memory range for each subgroup ; when in OFF position there is no selection.

The ten position switch (WINDOWS) permits to select window irrespective of the selection made with the switches. It is used during controls or calibration. With the switch in OFF, the full PIF spectrum is collected ; when in SEL the output signals are classified according to the eight switches selection.

The TEST/MEASURE switch is for a simple and fast window adjustement as will be described in Section 5.

In the rear two multipolar connectors are present : the former for SAMP and IDENT input pulses from the identifier ; the latter for digital output to the ADC.

Let us follow the block diagram of Fig. 9. The comparators are provided with two inputs : the first one is biased by a stabilized voltage of about 6 V. The second one is fed with a signal entering the eight comparators at the same time and selected by means of the TEST/MEASURE switch. On MEASURE, the PIF signal from the identifier enters the comparators ; the same pulse, analogically decoupled, feeds the front IDENT connector ; on TEST a saw-tooth ramp generator feeds the input (see Section 5).

During the computing, in order to minimize the total dead time, the eight thresholds are settled by suitably biasing the eight D-latch inputs. These are fed with a clock triggered by the sampling signal from the rear connector.

The D-latches are coded by means of a binary encoder that addresses only the highest comparator interested by the PIF signal. Such address, decoded in octal, allows the output of the corresponding sampling signal.

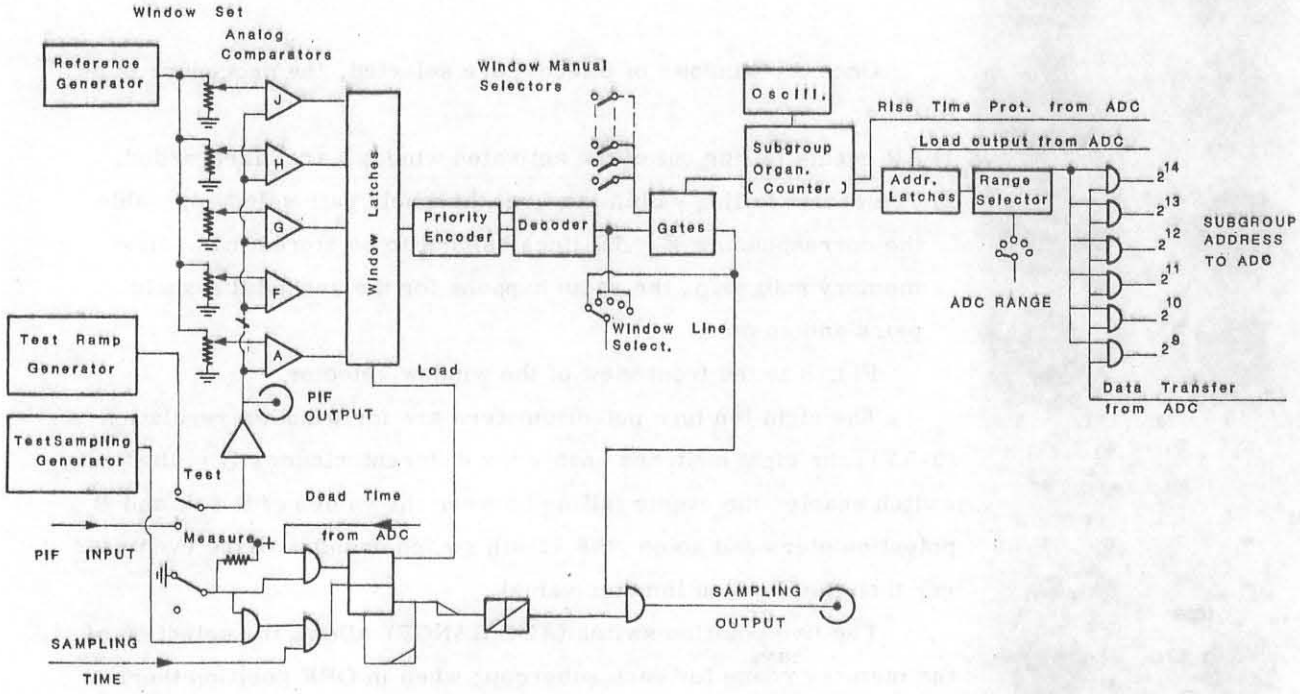

FIG. 9 - Block diagram of the window selector unit.

The working mode of the ADC RANGE switch will now be described. The subgroup selection is made by means of the word bits not used for the $E + \Delta E$ data, to obtain a correct labeling of different subgroups. It is necessary to decide, a priori, the number of bits reserved to the label. This requirement is satisfied through the ADC RANGE switch, that suitably chooses and transfers the label bits, via the rear connector.

The threshold D-latches go in exclusive or with the eight selection switches and charge a shift register in connection with the RTP of the ADC.

Taking out the data from the shift register at a 5 MHz frequency, it is possible to know how many enabled windows are interested by the PIF pulses. Evaluating the number of these windows, one gets, on the counter, the binary address of the inspected subgroup. The timing diagram of the selector waveform is shown in Fig. 10.

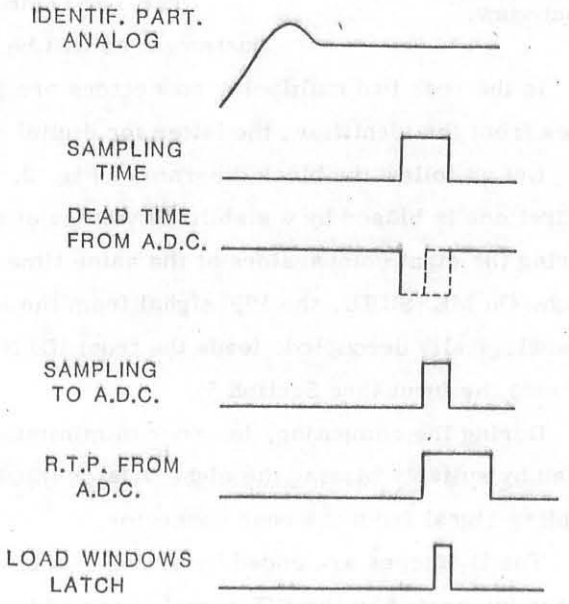

FIG. 10 - Timing of waveform in window selector.

5. - SETTING UP PROCEDURE.

For semplicity purpose, let us consider an experimental set up as sketched in Fig. 3. We will disregard, at the moment, the $\bar{E}$ and γ signals as they do not affect the general operating mode of the identifier. The E and ΔE pulses from the telescope, through a conventional amplification chain, enter directly the identifier. First, the gains of the two channels E and ΔE are balanced using, for example, an α source. Each signal, from one or the other detector, appears on the linear output connector: E with no ΔE input and with the coincidence mode selector in E; viceversa for ΔE. To check the E - ΔE time coincidence, one looks at the pulses at the test point base. The time coincidence is adjusted by means of the two DELAY potentiometers. With the coincidence mode selector on E ΔE, the outputs SAMP and E+ ΔE give the energy spectrum of all the reaction products, while SAMP and IDENT give the PIF spectrum.

Using the same signals from the window selector, with switch on MEASURE, it is possible to mark, on the display of the data acquisition system, the ranges for different group of particles. The window adjustment in beam, at a low counting rate, may be very long: the operation is shortened with the switch on TEST. In fact, having collected a PIF spectrum with a number of counts just enough to set the limits for different particles, off beam, switching on TEST, the saw-tooth ramp generator starts instead of the PIF signal. It covers the entire range (0-4 V) at a high counting rate ($\simeq$10 KHz) and the window position may be fixed very easily.

Now, the memory range for the energy spectra may be chosen, by means of the ADC RANGE switch. The system is ready for spectra acquisition, using the E+ ΔE signal from the identifier and the sampling from the selector.

If a reject signal $\bar{E}$ is used, only the gate threshold has to be adjusted.

When the γ-coincidence is wanted, the γ-line of interest is selected using the sampling signals as input to the delayed coincidence of an ADC, whose linear input is fed by the γ-channel amplifier output; the coincidence mode selector has to be on γ. The measurement is made with the selector in E $\Delta E/\gamma$.

The off beam adjustement of the exponent and the optimization of the identifier operating conditions are possible and easy, using the special pulser DAG[5], as it will be shown in next Section.

6. - EXPERIMENTAL RESULTS.

The operation of the identifier has been tested in two ways: off beam, simulating experimental conditions, and in beams. In the first case, the DAG generator has been used to simulate the following reactions: $^{27}Al(p,p')^{27}Al$, $^{27}Al(p,d)^{26}Al$, $^{27}Al(p,t)^{25}Al$, $^{27}Al(p,{}^{3}He)^{25}Mg$, $^{27}Al(p,\alpha)^{24}Mg$ at incident proton energy E_p = 36 MeV, and detecting angle $\theta_{lab} = 30^{o}$. The ΔE detector is assumed 100 μm thick, the particle stopping power in Si are from ref. (6).

The considered energy range extends from the thin detector energy cut-off to the maximum allowed by kinematics.

In Fig. 11 is reported the identification spectrum for the five simulated particles, obtained with x = 1.73.

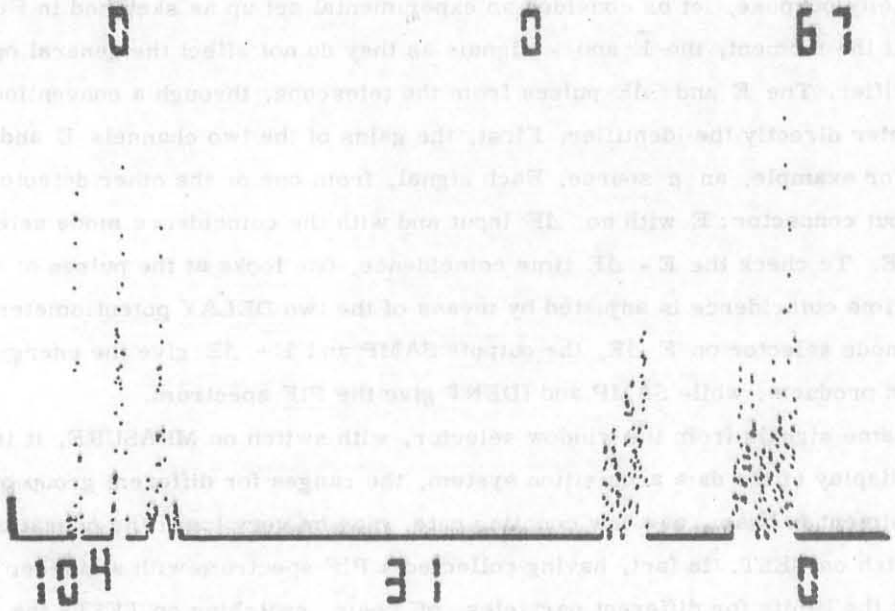

FIG. 11 - Mass identification spectrum simulated with the DAG Pulser.

The in beam test, with the same reactions, has been made at the Milan University AVF Cyclotron, at an incident proton energy E_p = 30 MeV.

A natural Al target (600 $\mu g/cm^2$ thick) and a Si detector telescope (150 + 5000 μm thick) were used. The exponent was set at the value obtained in the simulated experiment (x = 1.73).

The identification spectrum, at $\theta_{lab} = 30^o$, is shown in Fig. 12. In Figs. 13 are reported

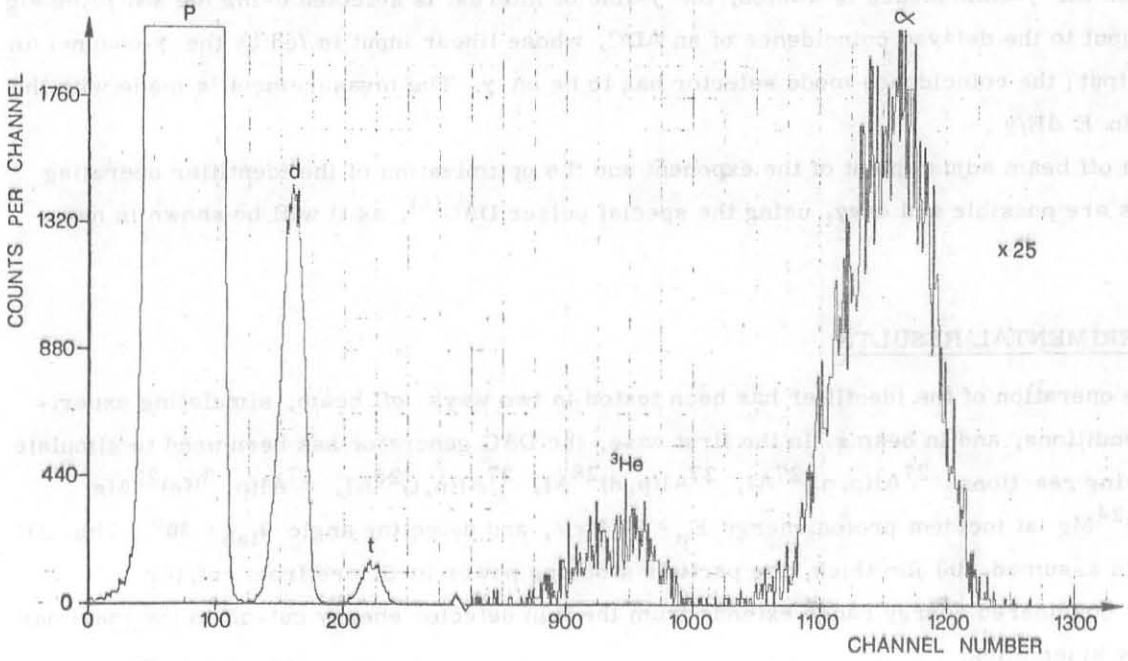

FIG. 12 - Mass identification spectrum obtained with proton beam.

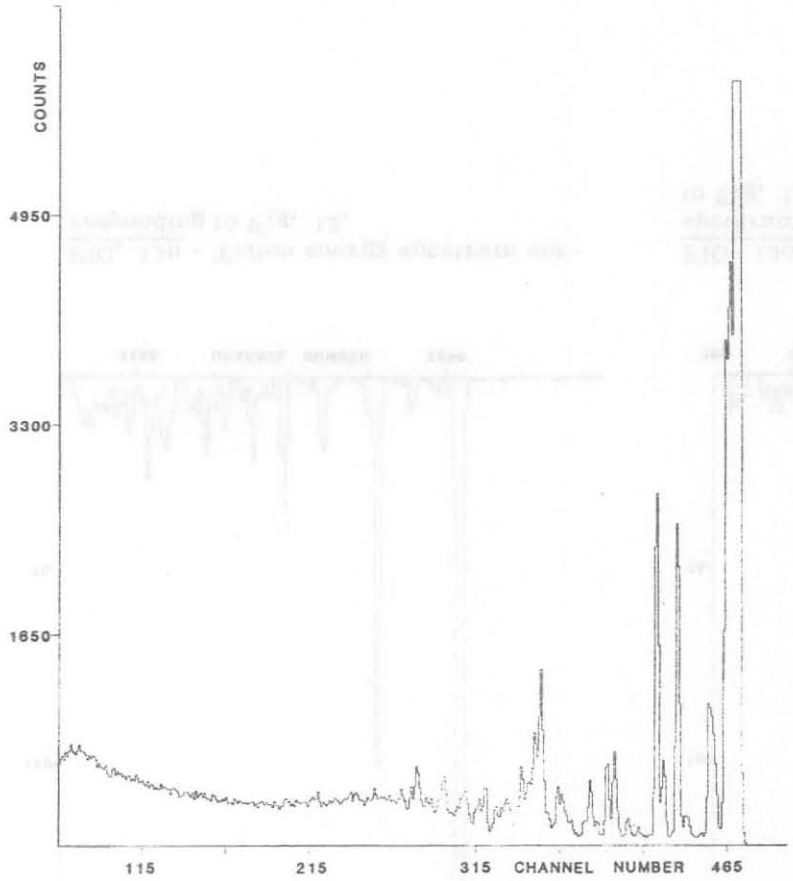

FIG. 13a - Proton energy spectrum corresponding to Fig. 12.

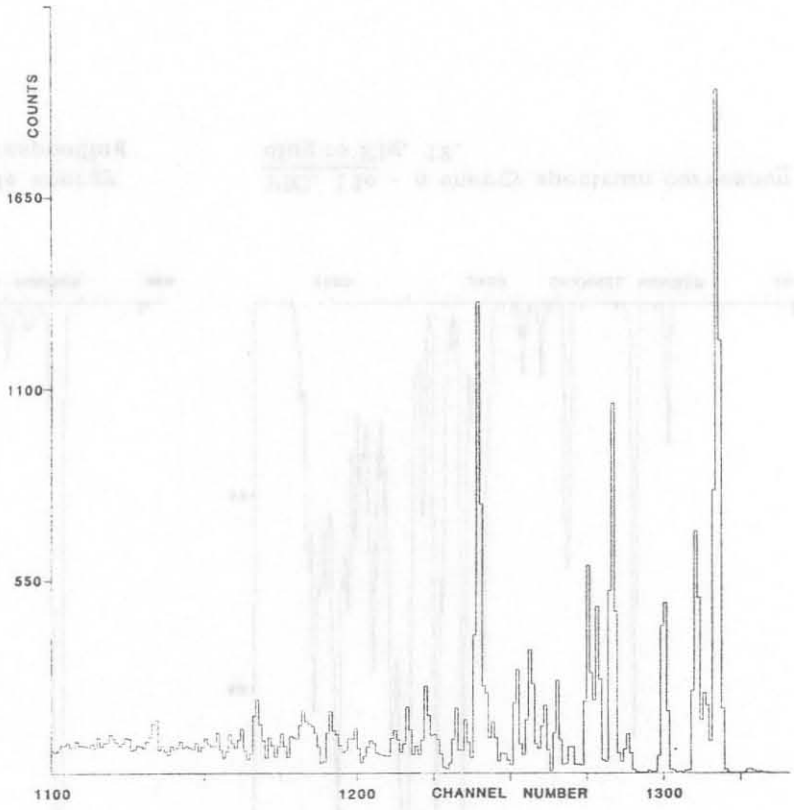

FIG. 13b - Deuteron energy spectrum corresponding to Fig. 12.

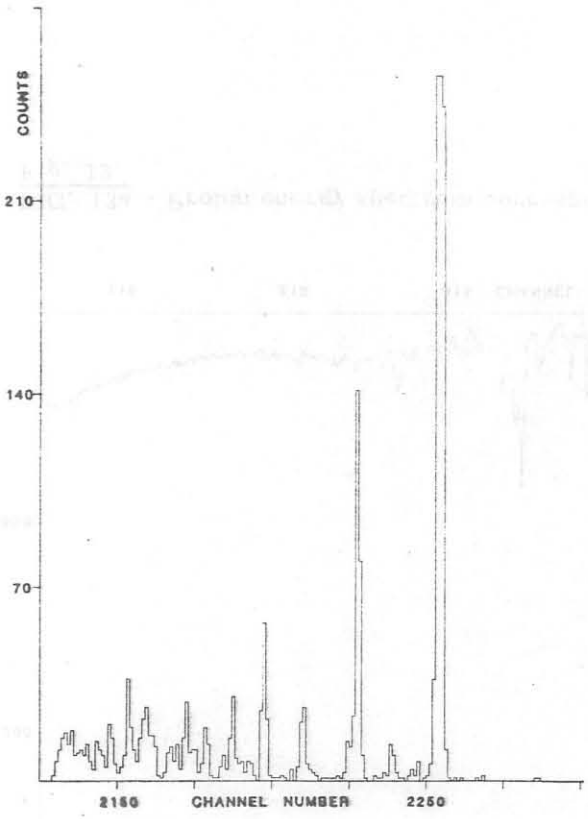

FIG. 13c - Triton energy spectrum corresponding to Fig. 12.

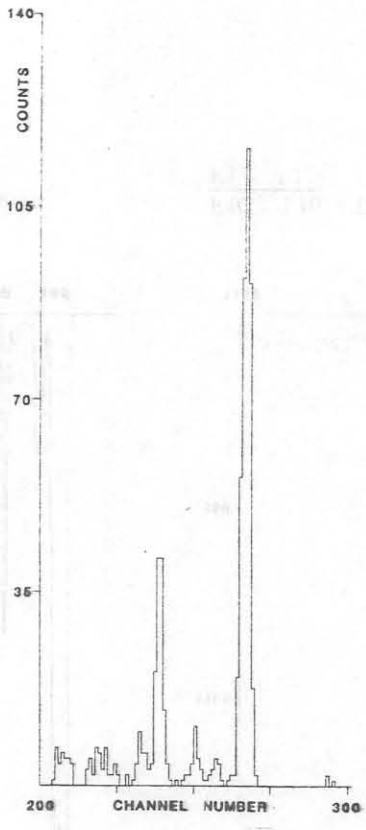

FIG. 13d - ^{3}He energy spectrum corresponding to Fig. 12.

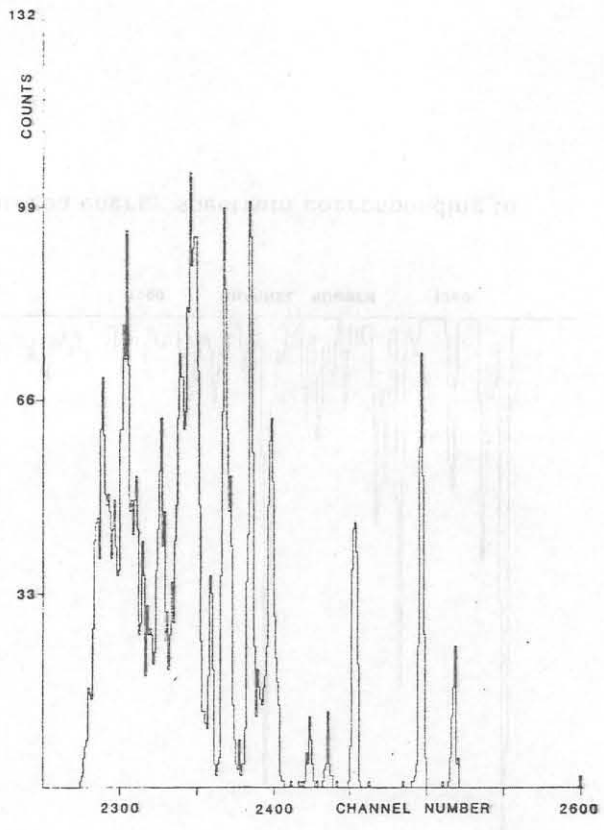

FIG. 13e - α energy spectrum corresponding to Fig. 12.

the energy spectra of the five different particles. The minimum detected energy is the ΔE cut-off. The mass discrimination obtained is good; it is worthwhile noticing that:

a) no in beam exponent adjustment was required;

b) the energy spectra extended over a pretty large energy range (about 28 MeV for protons).

As an example of very good mass discrimination obtainable, in Fig. 14 is shown the mass spectrum for ^3He and α from $(p+^{27}Al)$ at $E_p = 40$ MeV and $\theta_{lab} = 30^\circ$. It has been obtained with an ad hoc choice of the thin detector (50 μm), that gives better result but, of course, limits the kind of detectable particles. In this case the E detector was 2000 μm thick and a reject $\overline{E}$ detector (1000 μm) was used to minimize the proton background. The corresponding energy spectra are in Figs. 15.

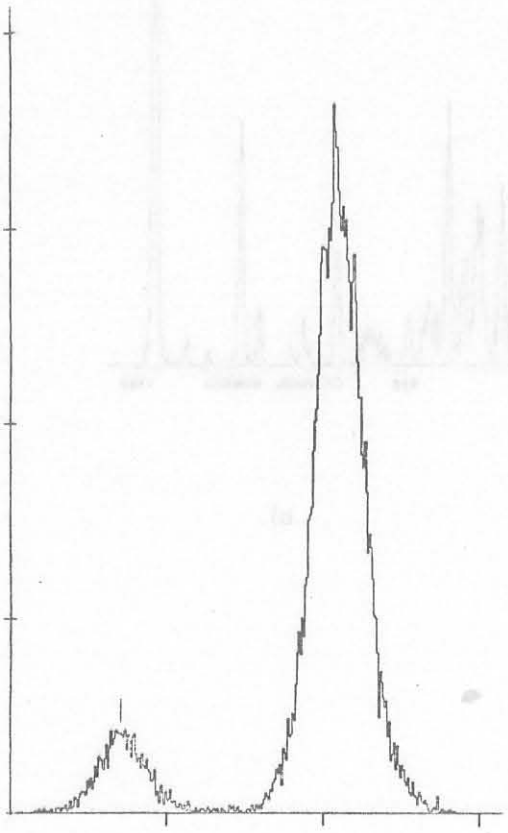

FIG. 14 - ^3He and α mass identification spectrum.

To check the correct mass discrimination, three-dimensional spectra of p, d, t were collected (Figs. 16), for the reactions $(p+^{90}Zr)$ at $E_p = 44.4$ MeV and $\theta_{lab} = 30^\circ$. The ΔE thickness (250 μm) was chosen to prevent ^3He and α detection.

The identifier efficiency was tested, in a simulated experiment, also for particles with $Z = 3$, i.e. Li ions. With the DAG pulser, the reactions $^{27}Al(^6Li, ^6Li)^{27}Al$ and $^{27}Al(^6Li, ^7Li)^{26}Al$, at 45 MeV incident energy and $\theta_{lab} = 30^\circ$, were simulated: the mass spectrum is shown in Fig. 17. The ΔE detector was assumed 30 μm thick; the stopping powers for Li ions in Si are from ref. (7). The ions energy covers a wide range of about 40 MeV; the discrimination for the entire energy range has been optimized varying the exponent[4], finally settled at $x = 1.66$.

Fig. 18 is an example of a γ-particle coincidence spectrum obtained with a mixed nuclides α source (^{239}Pu, ^{241}Am, ^{244}Cm). The two spectra are reported: the one without and the other with γ-coincidence.

The acquisition time was 160000 s for the γ-coincidence spectrum and 3000 s for the other. The selected 60 keV γ-line[8] was detected with a Ge(Li) detector.

In the γ-coincidence spectrum, one notices only two peaks, corresponding to ^{241}Am α particles of 5442 and 5484 keV. No α emission coincident with 60 keV γ-line, from ^{239}Pu or ^{244}Cm is present: the few counts in the γ-coincidence spectrum (except of course for ^{241}Am), are due to random coincidence.

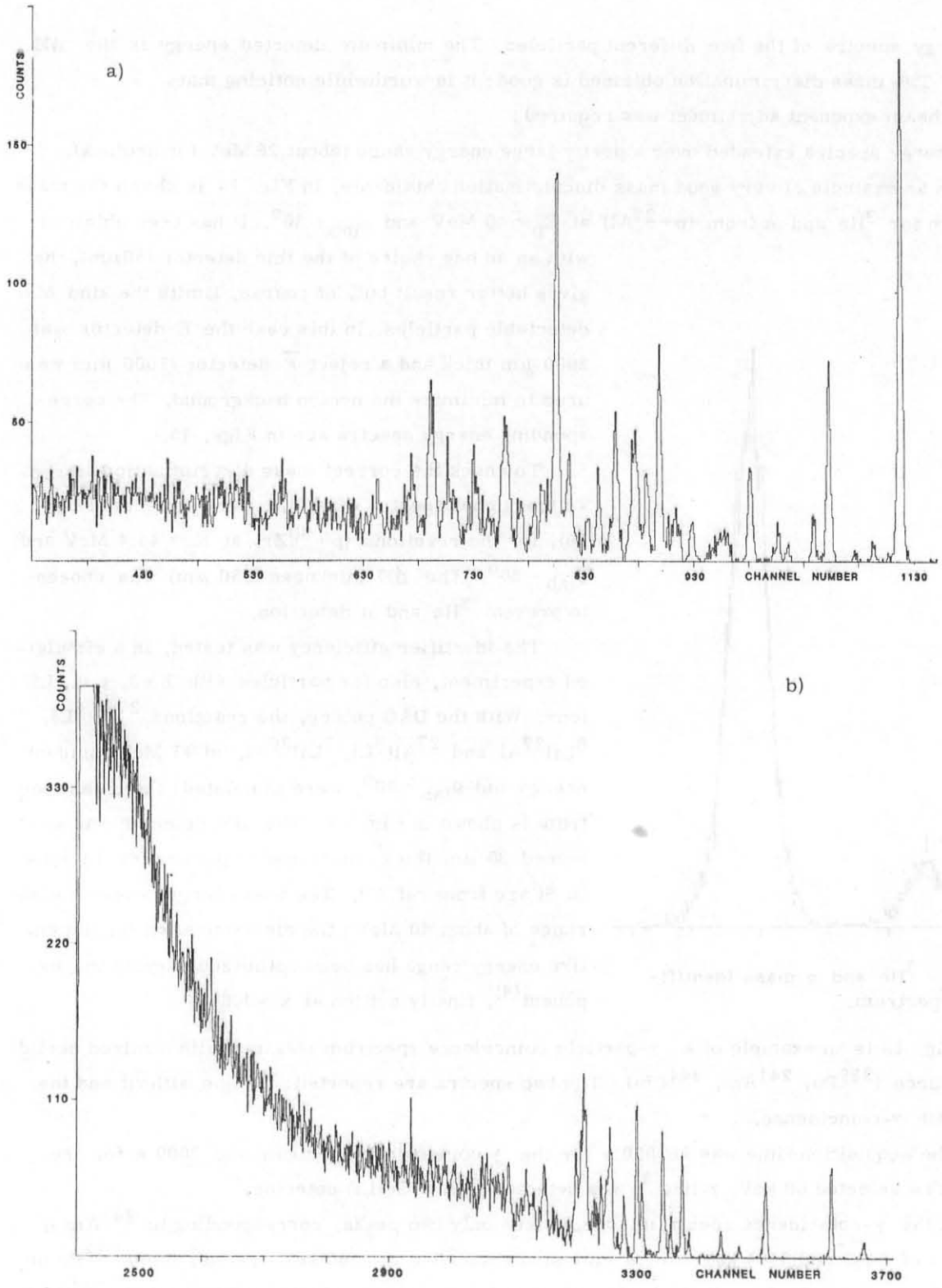

FIG. 15 - a) ^{3}He energy spectrum corresponding to Fig. 14; b) α energy spectrum corresponding to Fig. 14.

a)

b)

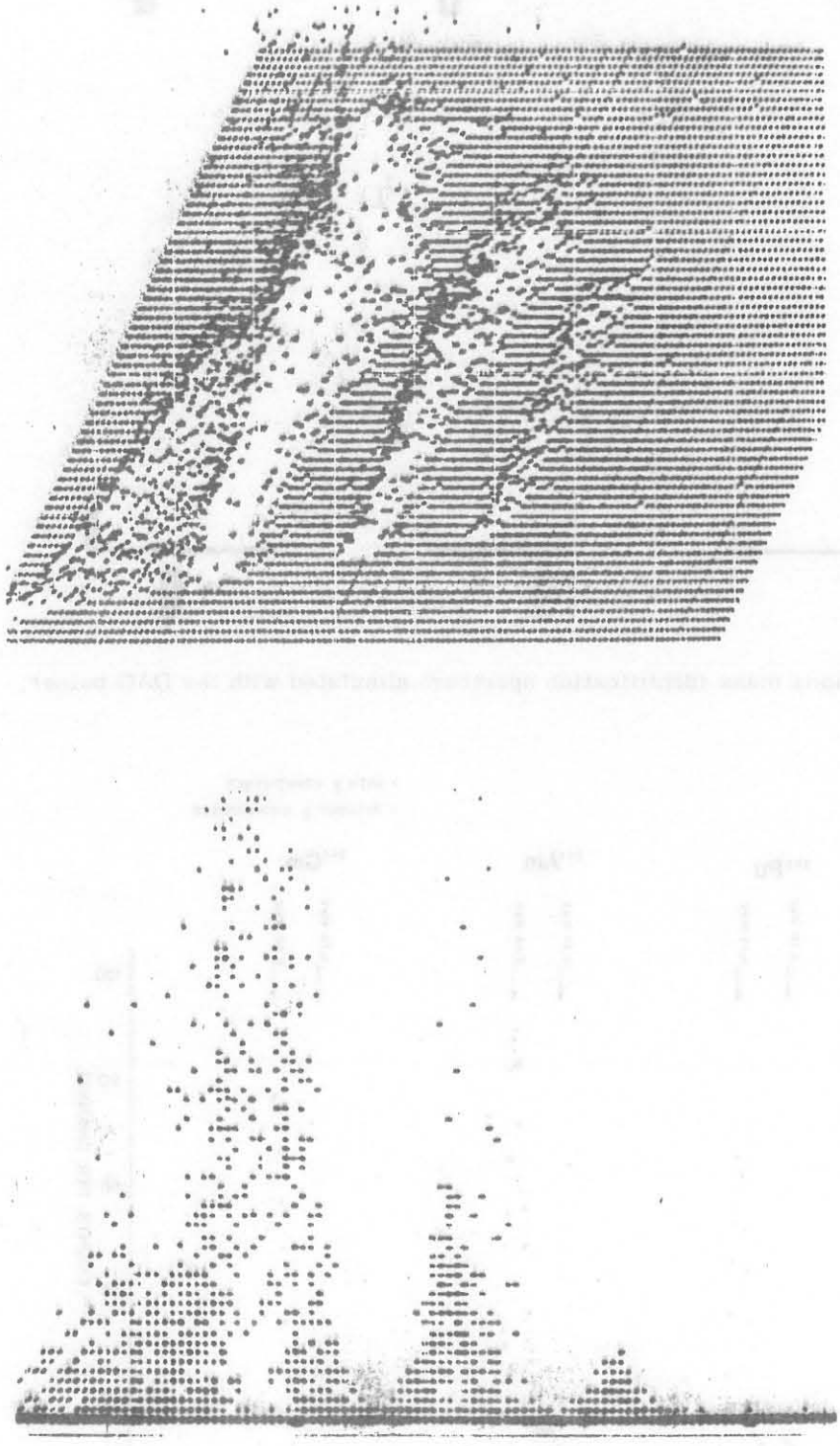

FIG. 16 - a) Photograph of a three-dimensional display of $(E + \Delta E)$ vs PIF (see text); b) The same, projected on the PIF axis.

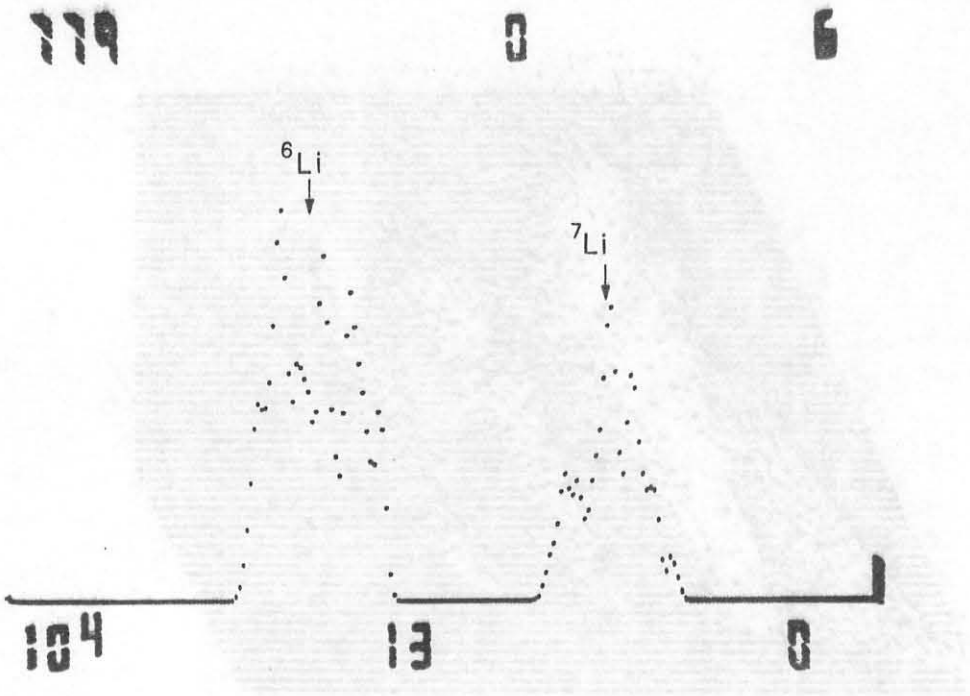

FIG. 17 - Li ions mass identification spectrum simulated with the DAG pulser.

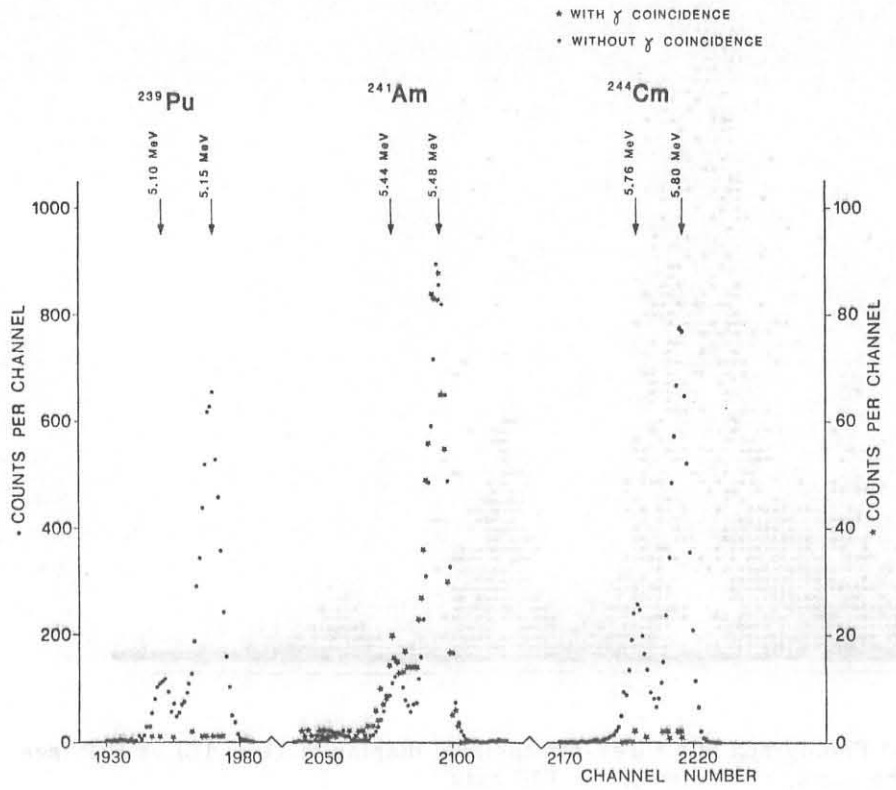

FIG. 18 - α-γ coincidence spectrum (see text).

REFERENCES.

(1) - F. S. Goulding and B. G. Harvey, Ann. Rev. Nucl. Sci. 25, 167 (1975), and references therein.

(2) - F. S. Goulding, Nuclear Instr. and Meth. 162, 609 (1979).

(3) - F. S. Goulding, D. A. Landis, J. Cerny and R. H. Pehl, Nuclear Instr. and Meth. 31, 1 (1964).

(4) - J. Cerny, S. W. Cosper, G. W. Butler, H. Brunnader, R. L. Mc Grath and F. S. Goulding, Nuclear Instr. and Meth. 45, 337 (1966).

(5) - P. Guazzoni, P. Michelato, A. Moroni, G. F. Taiocchi and L. Zetta, Nuclear Instr. and Meth. 185, 219 (1981) ; and Report INFN/BE-80/9 (1980).

(6) - J. Picard and G. Souchère, Rapport CEA-R3371.

(7) - F. Hubert, A. Fleury, R. Bimbot and D. Gardes, Rapport IN2P3, CEN Gradignan, IPN Orsay.

(8) - C. M. Lederer and S. Shirley, Table of Isotopes (Wiley, 1978).